

# INFILTRATION/CURE MODELING OF RESIN TRANSFER MOLDED COMPOSITE MATERIALS USING ADVANCED FIBER ARCHITECTURES<sup>1</sup>

Alfred C. Loos and Mark H. Weideman  
Virginia Polytechnic Institute and State University

Edward R. Long, Jr.  
Langley Research Center

David E. Kranbuehl, Philip J. Kinsley and Sean M. Hart  
College of William and Mary

## SUMMARY

A model was developed which can be used to simulate infiltration and cure of textile composites by resin transfer molding. Fabric preforms were resin infiltrated and cured using model generated optimized one-step infiltration/cure protocols. Frequency-dependent electromagnetic sensing (FDEMS) was used to monitor in situ resin infiltration and cure during processing. FDEMS measurements of infiltration time, resin viscosity, and resin degree of cure agreed well with values predicted by the simulation model. Textile composites fabricated using a one-step infiltration/cure procedure were uniformly resin impregnated and void free. Fiber volume fraction measurements by the resin digestion method compared well with values predicted using the model.

## INTRODUCTION

Resin transfer molding (RTM) has been identified as a cost-effective manufacturing technique for fabricating damage tolerant composite structures with geometrically complex reinforcements. Dry textile preforms are infiltrated with resin and cured in a single step process thus eliminating separate prepreg manufacture and ply-by-ply layup. The number of parameters which must be controlled during infiltration and cure make trial and error methods of process cycle optimization extremely inefficient. Analytical processing models combined with in situ monitoring sensors are a superior alternative for the determination of optimum processing cycles.

In this paper a finite element model is presented which can be used to simulate one-dimensional, through-the-thickness, nonisothermal infiltration and cure of resin into a fabric preform. Compaction and permeability characteristics of the fabric preform along with the kinetic and viscosity characteristics of the thermosetting resin are incorporated into the model to predict, as a function of applied temperature and pressure boundary conditions, the following parameters: a) initial resin mass; b) resin front position and time required for preform infiltration; c) resin viscosity and degree of cure; and d) final part thickness and fiber volume fraction.

Textile composites were fabricated by RTM using model generated processing cycles. During fabrication, frequency dependent electromagnetic sensors (FDEMS) were used to monitor in situ infiltration time, resin viscosity, and resin degree of cure. The fabricated panels were C-scanned and cut into specimens for photomicrographs, fiber volume fraction measurements and mechanical testing. Measured values of infiltration time, resin viscosity and degree of cure, and fiber volume fraction, were compared with model predictions.

<sup>1</sup>This work was made possible through the support of the National Aeronautics and Space Administration-Langley Research Center grant no. NAG1-343 with Virginia Tech and grant no. NAG1-237 with the College of William and Mary.

## PREFORM CHARACTERIZATION

Infiltration is the process by which a fluid permeates a porous material. Infiltration is dependent on the applied pressure, the viscosity of the fluid, and the geometry of the solid micro-structure.

Infiltration into a simple rectangular preform can be accomplished either through the thickness or in-plane. With more complex three-dimensional materials, infiltration could occur in many directions at once. This study has been limited to one-dimensional, through-the-thickness infiltration of a rigid porous material.

Application of the pressure causes the preform to deform. The deformation is due to a combination of tow deformation, nesting of the plies, and flattening of individual layers. The changes in size and geometry of the interstitial spaces affect the rate of infiltration.

The internal structure of a porous material can be described by the porosity and permeability of the material. The porosity is the maximum volume of resin that a porous material can contain divided by the total volume and can be related to the solid volume fraction  $\nu_f$  by the following expression,

$$\phi = 1 - \nu_f \quad (1)$$

As the compaction pressure is increased, the porosity will decrease. Relationships between applied pressure and porosity and porosity and permeability are required to completely characterize a fabric preform and as input into the simulation model. Only a brief summary of the techniques used to determine these relationships will be presented. A detailed documentation of the experimental procedures is given in reference 1.

### Pressure-Porosity Relationship

Following the approach of Guavin, Chibani and LaFontaine (ref. 2) the fabric areal weight  $\xi$ , can be defined as the mass of fabric per unit surface area. The porosity can then be written as,

$$\phi = 1 - \frac{n\xi}{t\rho_{\text{solid}}} \quad (2)$$

where  $t/n$  is the thickness of one ply, and  $\rho_{\text{solid}}$  represents the density of the fibers. The values of  $\xi$  and  $\rho_{\text{solid}}$  are typically supplied by the fabric manufacturer.

One-dimensional compression tests were performed to characterize the deflection of various fabric preforms. Specimens were placed in a fixture, and then loaded in compression. The load was applied by an Instron multiaxial testing machine and the deflection of the preform was measured by a LVDT attached to the lower actuator. Data was recorded via an IBM PC during the loading and unloading cycles.

The measured data was described by a polynomial of the form,

$$d = a_1 + a_2 \ln P + a_3 (\ln P)^2 + a_4 (\ln P)^3 + a_5 (\ln P)^4 \quad (3)$$

where  $d$  is the deflection of the fiber bed and  $P$  is the compaction pressure. A nonlinear least squares procedure was used to determine the coefficients  $a_1$ ,  $a_2$ ,  $a_3$ ,  $a_4$  and  $a_5$ . Substituting equation (3) into equation (2) the relationship between pressure and porosity is obtained. Figure 1 represents the pressure–porosity relationship for an eight harness satin fabric woven from Hercules IM7 fibers (IM7/8HS). As expected the porosity decreases with increasing compaction pressure.

### Permeability–Porosity Relationship

The permeability of a porous material can be experimentally determined using D'Arcy's law. The one–dimensional form of D'Arcy's law can be written as

$$q = K \frac{A \Delta P}{\mu t} \quad (4)$$

where  $q$  is the volumetric flow rate,  $K$  is the permeability,  $A$  is the area normal to the flow direction,  $\mu$  is the fluid viscosity, and  $\Delta P$  is the pressure differential across the material.

An experimental program was implemented to determine the through–the–thickness permeability of fabric preforms. The fixture used to measure the permeability of a fabric preform is shown schematically in figure 2. The fixture allows constant compaction pressures to be applied independent of the pressure gradient.

To measure the permeability of the preform, the fabric was compressed to a known thickness and constant flow conditions were established. The flow through the preform was measured with a bubble–type flow meter, and the pressure drop was measured. Tap water was used in all tests.

Flow results from twelve plies of IM7/8HS are shown in figure 3. The flow rate behaves in a linear fashion with respect to the pressure gradient indicating D'Arcy's law is applicable to flow through fabric preforms. From the slope of the experimental curves, the permeability of the porous material can be determined as follows,

$$\text{Slope} = \frac{q}{\frac{\Delta P}{t}} = K \frac{A}{\mu} \quad (5)$$

The effect of the compaction pressure is clearly evident from the changing slope of the data. As the pressure on the material increases, the interstitial spaces become smaller, which increases the resistance to flow and decreases the permeability.

For fibrous materials the Kozeny–Carman relation has been used to relate permeability to porosity, and can be written as follows:

$$K = \frac{d_f^2}{\kappa} \frac{\phi^3}{(1 - \phi)^2} \quad (6)$$

where  $d_f$  is the fiber diameter and  $\kappa$  is the Kozeny–Carman coefficient which must be determined experimentally.

The measured permeability versus porosity for the first loading cycle of an IM7/8HS fabric is shown in figure 4. From the figure it can be seen that as the compaction pressure increases, the porosity decreases with a corresponding decrease in permeability. The solid line plotted on figure 4 was obtained from the Kozeny–Carman equation when  $\kappa = 38.8$ .

### INFILTRATION/CURE SIMULATION MODEL

The compaction characteristics, pressure–porosity relationship, and Kozeny–Carman equation were combined with D’Arcy’s law and an unsteady heat transfer analysis to produce a comprehensive model of the infiltration and cure of a viscous resin into a fabric preform. Also included in the model formulation are cure kinetics and viscosity models to calculate the advancement of the resin and the changes in viscosity with resin advancement during infiltration and cure. The model was developed to simulate one–dimensional, through–the–thickness infiltration. Solution of the governing equations was obtained using the finite element technique. The infiltration/cure model is shown diagrammatically in figure 5. A detailed description of the model formulation and numerical procedures is given in reference 1.

For a specified compaction pressure and temperature cure cycle, the model can be used to predict the following parameters during infiltration and cure: a) initial resin mass; b) resin front position and preform infiltration time; c) preform temperature distribution; d) resin viscosity and degree of cure; and e) final part thickness and fiber volume fraction.

### FREQUENCY DEPENDENT ELECTROMAGNETIC SENSING (FDEMS)

In studies of epoxies, polyimides, phenolics and unsaturated polyesters, frequency dependent electromagnetic sensing (FDEMS) has been shown to be a convenient automated instrumental technique for monitoring in situ the processing properties of these thermoset resins continuously throughout the cure process. FDEMS is able to monitor the progress of cure including reaction onset, point of and magnitude of maximum flow, fluidity, solvent evolution, buildup in modulus, approach to T<sub>g</sub>, reaction completion and degradation (refs. 3–9). FDEMS measurements are particularly useful as they can be conveniently made both in a laboratory and in situ in the tool during processing in the fabrication environment. Measurements are made continuously throughout the entire fabrication cycle. Further, FDEMS provides a convenient computerized method for recording, storing, and comparing resin processing properties throughout cure. As such FDEMS can be used to evaluate and control resin properties prior to use, to provide a signature verifying the cure process during fabrication, and to provide in situ sensor feedback for intelligent closed loop control of fabrication.

#### Theory

Measurements of the capacitance, C, and conductance, G, were made using a Dek Dyne FDEMS sensor. The complex permittivity  $\epsilon^* = \epsilon' - i\epsilon''$  was calculated from

$$\epsilon' = \frac{C \text{ material}}{C_0} \quad (7)$$

and

$$\epsilon'' = \frac{G \text{ material}}{C_0 2\pi f} \quad (8)$$

at each of 10 frequencies between 50 Hz and 1 MHz. This calculation is possible when using the

Dek Dyne sensor whose geometry independent capacitance,  $C_0$ , is invariant over all measurement conditions.

Both the real and the imaginary parts of  $\epsilon^*$  have an ionic and dipolar component. The dipolar component arises from diffusion of bound charge or molecular dipole moments. The dipolar term is generally the major component of the dielectric signal at high frequencies and in highly viscous media. The ionic component often dominates  $\epsilon^*$  at low frequencies, low viscosities and/or higher temperatures.

Simultaneous measurement of the frequency dependence of both  $\epsilon'$  and  $\epsilon''$  or C and G in the Hz to MHz range is, in general, optimum for determining both the ionic mobility or conductivity,  $\sigma$ , and a mean dipolar relaxation time,  $\tau$ . These two parameters are directly related on a molecular level to the rate of ionic translational diffusion and dipolar rotational mobility and thereby to changes in the molecular structure of the resin which reflect the reaction rate, changes in viscosity – modulus, and the degree of cure.

### Instrumentation

The Dek Dyne FDEMS sensor was developed as an inert, disposable, planar, geometry-independent microsensors system. The sensor consists of only a fine array of two interdigitated comb electrodes. Further, the sensor is constructed from noble metals and high temperature ceramics and does not contain solid state circuitry, which is vulnerable to the harsh processing environment. The sensor is designed to withstand the curing/tool temperature, pressure, and oxidative conditions during processing for temperatures exceeding 400° C and pressures of 1 MPa. This single disposable sensor is capable of monitoring simultaneously the entire range in magnitude (usually  $10^{-2} - 10^8$ ) of both the real  $\epsilon'$  and imaginary  $\epsilon''$  components of the permittivity continuously without interruption throughout the cure cycle. The sensor and the accompanying software are designed for modular use with commercially available advanced impedance and conductivity bridges.

## EXPERIMENTAL

### Composite Fabrication

Textile composites for this program were fabricated from Textile Technologies, Inc. eight harness satin fabric woven from Hercules IM7 graphite fibers (TTI 8HS/IM7) and Hercules 3501-6 epoxy resin. Sixteen ply, 15.2 cm x 15.2 cm fabric preforms were resin infiltrated and cured using the mold assembly shown in figure 6. The advantage of this technique is that fabric preforms can be infiltrated and cured in a one step process using a heated platen press. A 15.2 cm x 15.2 cm resin panel is made in a separate step prior to fabrication of the composite. The amount of resin required to produce a composite with a specified fiber volume fraction can be calculated using the infiltration/cure model. For hot melt resin systems, the resin panel must be completely degassed prior to fabrication of the composite. This is a key step and will ensure production of a void free laminate.

During layup, two FDEMS sensors and two type J thermocouples were placed inside the mold. A sensor and thermocouple were each placed on the bottom of the mold between the release film and the resin panel as shown in figure 6. A second sensor and thermocouple were each placed on top of the graphite fiber preform. Thus the bottom sensor was able to make continuous measurements of the state of the resin at the bottom of the mold below the fabric. The top sensor was able to monitor the time it takes for the resin to infiltrate to the top of the fabric and the state of the infiltrated resin at the top of the mold.

The mold assembly was vacuum bagged and placed between the upper and lower platens of the press. A full vacuum of 760 mm Hg and the platen compaction pressure were applied to the mold at the beginning of the process and held constant for the duration of the infiltration and cure cycle. The platens were then heated according to the prescribed temperature cure cycle. Thermocouples were mounted on the upper and lower platens to monitor the temperature.

During processing, the thermocouple temperatures and the multiple frequency FDEMS capacitances and conductances were measured and recorded using a computer controlled data acquisition system. The deflection of the plunger as a function of time was recorded with a dial gauge utilized to estimate the position of the resin infiltration front.

Upon completion of cure, the textile composite was C-scanned and the final weight and dimensions were recorded. The composites were cut into specimens for photomicrographs, fiber volume fraction measurements and mechanical testing. Fiber volume fraction measurements were made in accordance with the ASTM Test Method for Fiber Content of Resin-Matrix Composites by Matrix Digestion (D3171-76). Compression strength measurements were made using the short-block compression specimen configuration described in reference 10. A minimum of five specimens from each panel were tested.

## RESULTS AND DISCUSSION

### Infiltration/Cure Processing Cycles

For the investigation, four textile composite panels were fabricated using the one-step infiltration and cure technique described in the preceding section. Two panels were manufactured using the recommended cure cycle for Hercules 3501-6 resin preregs (see temperature cure cycle, figure 11). The remaining two panels were manufactured using a "rapid" cure cycle developed using the infiltration/cure model. In the rapid cure cycle, the composite is heated at 3.0° C/min from room temperature to the final hold temperature of 177° C. The intermediate hold has been eliminated and the final hold time has been reduced by 20 minutes. Two compaction pressures were used to produce composites with fiber volume fractions of 60% or 65%. The infiltration/cure model was used to calculate the compaction pressure required to fabricate a composite with the desired fiber volume fraction. For the TTI IM7/8H fabric, compaction pressures of 276 kPa and 551.5 kPa are required to fabricate composites with fiber volume fractions of 60% and 65%, respectively.

### FDEMS Measurements

Figure 7 is a plot of the loss factor  $\epsilon''$  multiplied by the frequency  $\omega$  measured by the bottom sensor (sensor 1, figure 6) during infiltration and cure using the manufacturer's recommended cure cycle. Figure 8 is a similar plot for the sensor placed at the top of the fabric preform (sensor 2, figure 6) during RTM using the model generated rapid cure cycle. Plots of  $\epsilon''$  multiplied by frequency ( $\epsilon'' \cdot \omega$ ) are recommended because they conveniently display the frequencies and times where  $\epsilon''$  is dominated by ionic diffusion. That is, overlapping lines of  $\epsilon''$  multiplied by frequency indicate the frequencies and time periods when  $\epsilon''$  is dominated by ionic diffusion. At these frequencies, the ionic mobility can be tracked through the specific conductivity  $\sigma$ . The specific conductivity is calculated from the ionic component of  $\epsilon''$  ( $\epsilon_1''$ ) and the frequency (f) using the following relationship:

$$\sigma = 8.854 \times 10^{-14} \cdot 2\pi \cdot f \cdot \epsilon_1'' \quad (9)$$

The relationship of  $\epsilon_1''$  or  $\sigma$  to viscosity and degree of cure was determined through a previous series of isothermal resin characterization runs in the laboratory using FDEMS sensors, differential scanning calorimetry, and dynamic mechanical measurements of viscosity. These runs were used to construct a look-up table which related the ionic mobility as tracked by  $\sigma$  for a particular temperature to the viscosity. A second independent look-up table was constructed relating  $\sigma$  for a given temperature to the degree of cure. These characterization matrices were used to determine the changing magnitude of the viscosity and the buildup in degree of cure at a particular position in the mold from the FDEMS sensor output.

The beginning of resin flow at the bottom of the mold (figure 7) and the time of resin infiltration to the top of the fabric preform (figure 8) are readily seen as the time at which the magnitude of  $\epsilon_1''$  jumps up several decades indicating resin wet out of the sensor.

### **Infiltration/Cure Model Simulations**

A comparison between the measured and calculated infiltration front position for the IM7/8HS preform infiltrated and cured using the manufacturer's cure cycle and the low compaction pressure is shown in figure 9. The infiltration front position was estimated by measuring the deflection of the mold plunger during infiltration. At early times there is some difference between the calculated and measured infiltration front position. This could be due to the fact that there are slight differences between the data used to develop the resin viscosity and fabric permeability models and the actual values used in the experiment. It is also possible that there are errors in the infiltration front measurement due to the small initial changes in mold plunger deflection. The bottom FDEMS sensor indicates that wet out and the beginning of infiltration occurs at about 26 minutes into the process (figure 7). If plunger deflection measurements are used, infiltration begins at 17 minutes into the process which is earlier than indicated by the FDEMS sensor measurements.

Comparisons between the calculated and measured infiltration times for the four composite panels manufactured are shown in figure 10. As can be seen from the figure there is very good agreement between the calculated and measured values. In all cases, the measured infiltration times are within 8% of the model predicted infiltration times.

For the composite panel fabricated using the rapid cure cycle and the high compaction pressure, the FDEMS sensor mounted at the top of the preform indicated wet out at 36 minutes (figure 8) which agrees well with the calculated and plunger deflection measured infiltration time.

The resin viscosity and degree of cure are shown in figures 11 and 12 for the manufacturer's cure cycle and in figure 13 and 14 for the rapid cure cycle. Agreement between the model predicted and the FDEMS sensor measured viscosity and degree of cure at the bottom of the preform (sensor 1, figure 6) is very good. With the rapid cure cycle, complete infiltration of the preform is easily achieved without the use of the intermediate hold period. Total cure time is reduced by almost 80 minutes.

Comparisons between the calculated and measured fiber volume fractions for the four textile composites are shown in figure 15. As can be seen from the figure the measured values of fiber volume fraction are within 5% of the model calculated values.

### **Mechanical Tests Results**

Results of the short block compression tests are shown in figure 16. The measured fiber volume fraction ( $\nu_f$ ) of each composite is denoted in the figure. The results show that the maximum compression stress at failure is slightly higher for the composites fabricated using the

rapid cure than for the composites fabricated using the manufacturer's cure cycle. It is interesting to note that the compressive strengths of the high volume fraction specimens are lower than the compressive strengths of the low volume fraction specimens. Photomicrographs of the high volume fraction specimens showed a fully infiltrated and well consolidated structure. However, high magnification photomicrographs did reveal a low percentage of micro-voids (void diameter on the order of filament diameter) which may have caused the slight reduction in compressive strength.

### CONCLUDING REMARKS

A process simulation model was developed for one-dimensional, through-the-thickness infiltration and cure of textile composites by resin transfer modeling. For a specified temperature cure cycle, the model was shown to accurately predict the required compaction pressure, initial resin mass, and time required to infiltrate a fabric preform to the desired fiber volume fraction. Frequency dependent electromagnetic sensing (FDEMS) was shown to be a convenient and accurate technique for in situ monitoring of resin infiltration and cure of a fabric preform. FDEMS sensors can be placed at different positions inside the fabric preform and used to monitor the resin fluidity and position of the resin front during infiltration and resin advancement during cure. With the proper calibrations, output of the FDEMS sensors can be directly related to resin viscosity and degree of cure for comparison with the predictions of the simulation model.

Textile composites for this investigation were manufactured using a newly developed one-step infiltration and cure technique. The non-autoclave process can be used to fabricate high quality textile composites to the desired fiber volume fraction.

### REFERENCES

1. Claus, S. J. and Loos, A. C.: A Cure Process Model for Resin Transfer Molding of Advanced Composites. Virginia Tech Center for Composite Materials and Structures., Report no. CCMS-89-07, Virginia Tech, Blacksburg, VA, April 1989.
2. Gauvin, R.; Chibani, M.; and Lafontaine, P.: The Modeling of Pressure Distribution in Resin Transfer Molding. *Journal of Reinforced Plastics and Composites*, vol. 6, Oct. 1987, pp. 367-377.
3. Kranbuehl, D.; Eichinger, D.; Loos, A.; and Long, E. R.: Sensor-Model Control of the Resin Transfer Molding Process. *Proceedings of the 48th SPE ANTEC Conference*, May 7-11, 1990, Society of Plastics Engineers, pp. 912-914.
4. Kranbuehl, D.: Cure Monitoring. *Encyclopedia of Composites*, S. M. Lee, ed., VCH Publishers, 1989, pp. 531-543.
5. Kranbuehl, D.; Delos, S.; Hoff, M.; and Haverty, P.: Use of Frequency Dependence of the Impedance to Monitor Viscosity During Cure. *Polymer Eng. & Sci.*, vol. 29, no. 5, May 1989, pp. 285-289.
6. Kranbuehl, D.; Hoff, M.; Haverty, P.; Loos, A.; and Freeman, T.: In-situ Measurement and Control of Processing Properties of Composite Resins in a Production Tool. *33rd International SAMPE Symposium*, vol. 33, 1988, pp. 1276-1284.
7. Kranbuehl, D.; Delos, S.; Hoff, M.; Weller, L.; Haverty, P.; and Seeley, J.: Dynamic Dielectric Analysis: Monitoring the Chemistry and Rheology During Cure of Thermosets. *ACS Division of Polymeric Materials: Science and Engineering*, vol. 56, 1987, pp. 163-168.

8. Kranbuehl, D.; Delos, S.; Hoff, M.; Weller, L.: Dynamic Dielectric Analysis: A Means for Process Control. 31th International SAMPE Symposium, vol. 31, 1986, pp. 1087–1094.
9. Kranbuehl, D. E.; Delos, S. E.; Yi, E. C.; Mayer, J. T.; Hou, T.; and Winfree, W.: Correlation of Dynamic Dielectric Measurements with Viscosity in Polymeric Resin Systems. 30th International SAMPE Symposium, vol. 30, 1985, pp. 638.
10. Dow, M. B. and Smith, D. L.: Properties of Two Composite Materials Made of Toughened Epoxy Resin and High-Strain Graphite Fiber. NASA Technical Paper 2826, July, 1988.

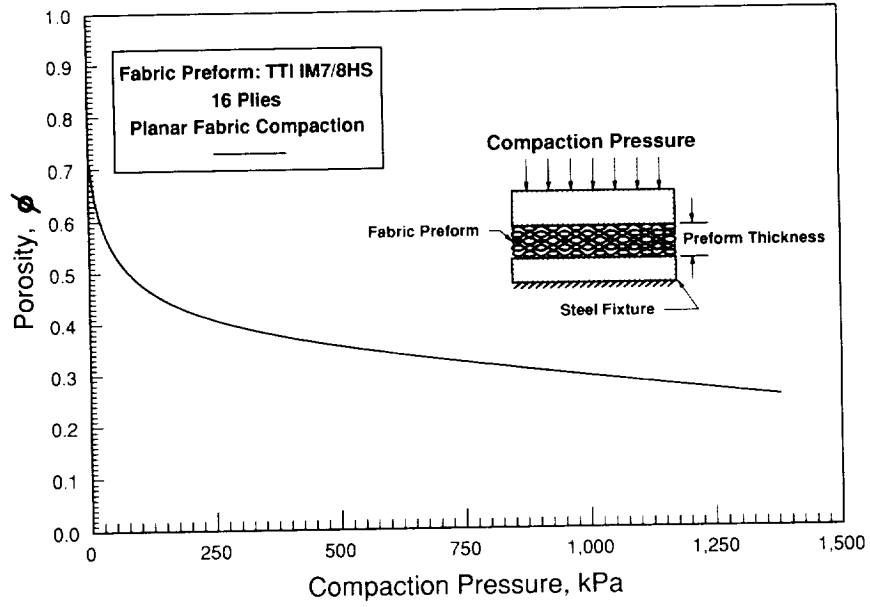


Figure 1. Relationship between porosity and compaction pressure for IM7/8HS woven fabric.

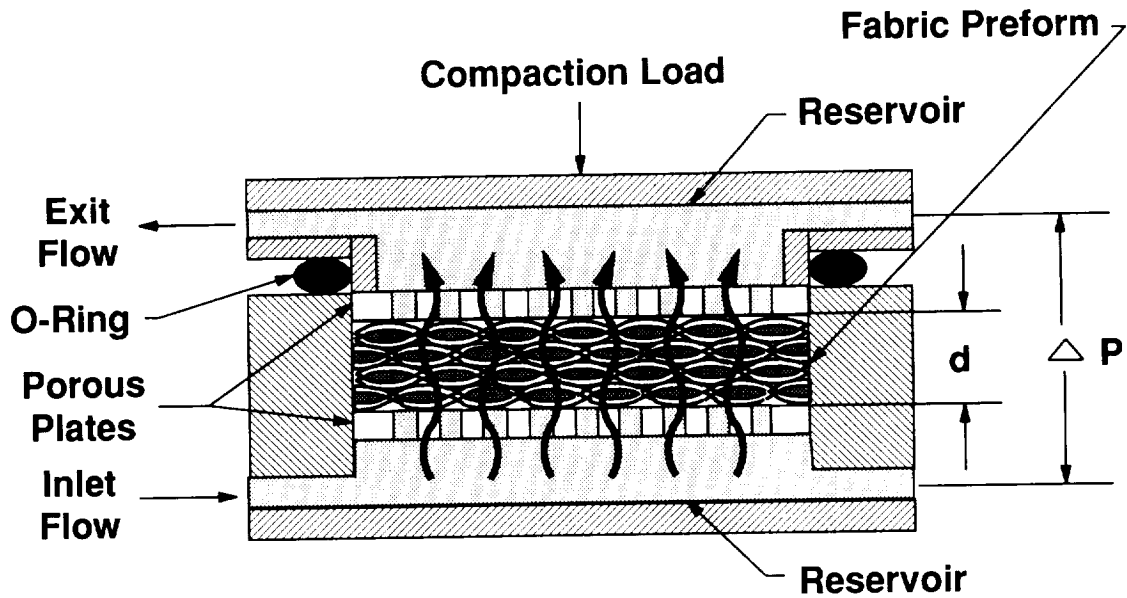


Figure 2. Schematic of the permeability test fixture.

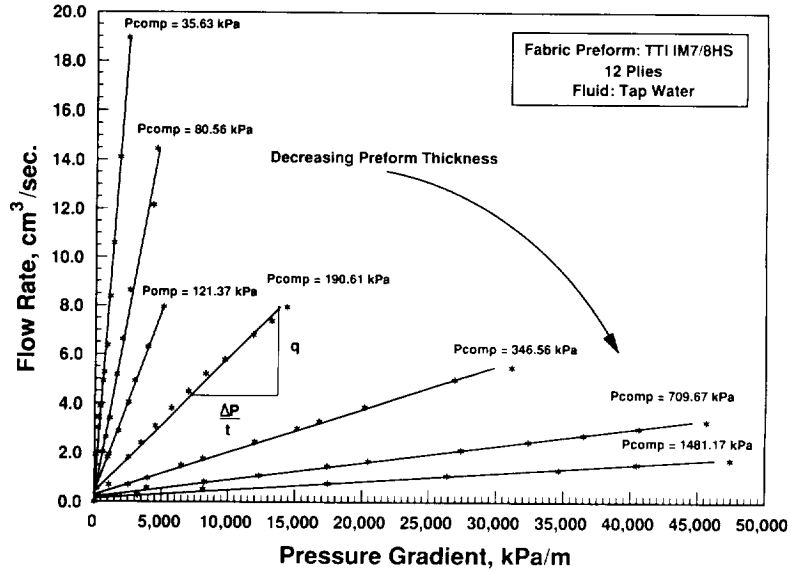


Figure 3. Flow rate–pressure gradient data for through–the–thickness flow of IM7/8HS woven fabric.

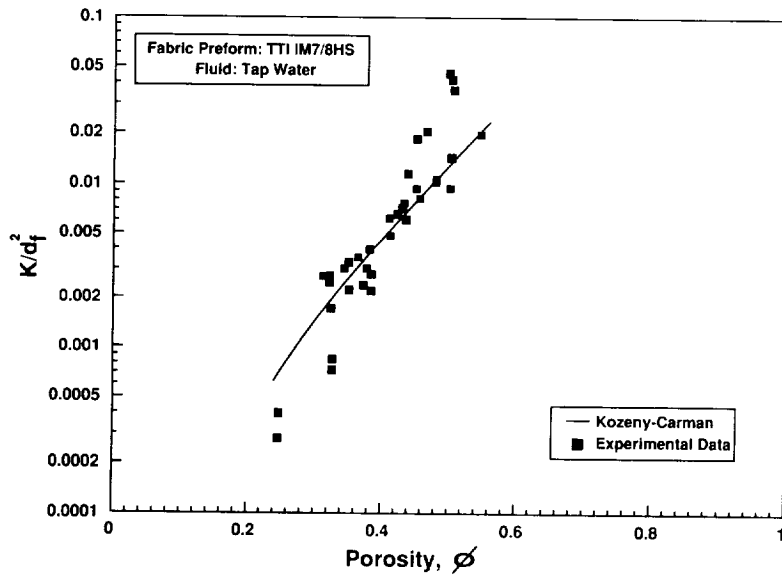


Figure 4. Normalized through–the–thickness permeability versus porosity for IM7/8HS woven fabric.

## RTM SIMULATION MODEL

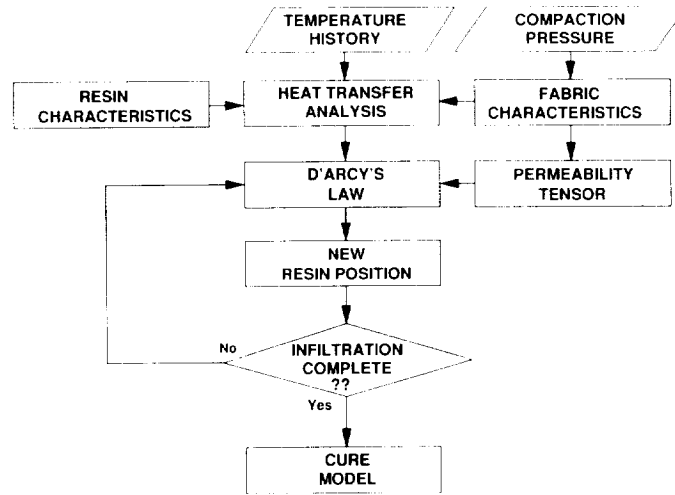


Figure 5. RTM simulation model.

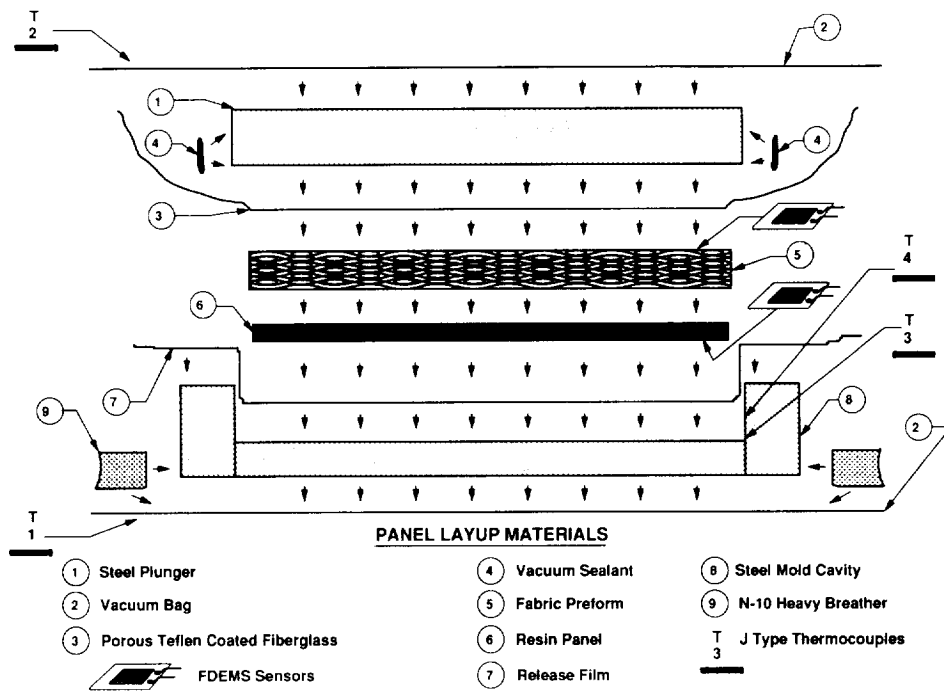


Figure 6. Schematic of the lay-up and mold assembly.

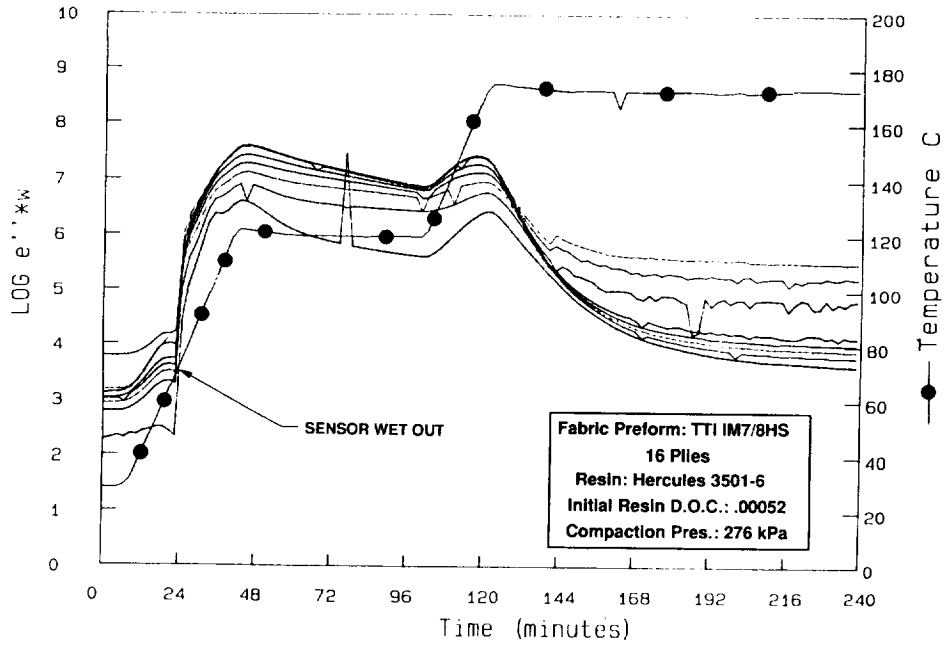


Figure 7. Values of  $\epsilon''$  multiplied by frequency ( $\epsilon'' \cdot \omega$ ) for the bottom sensor. Constant frequency lines plotted from bottom to top are 50 Hz, 125 Hz, 250 Hz, 500 Hz, 5 kHz, 25 kHz, 50 kHz, 0.25 MHz, and 0.50 MHz. Wet out of sensor occurs at 26 minutes.

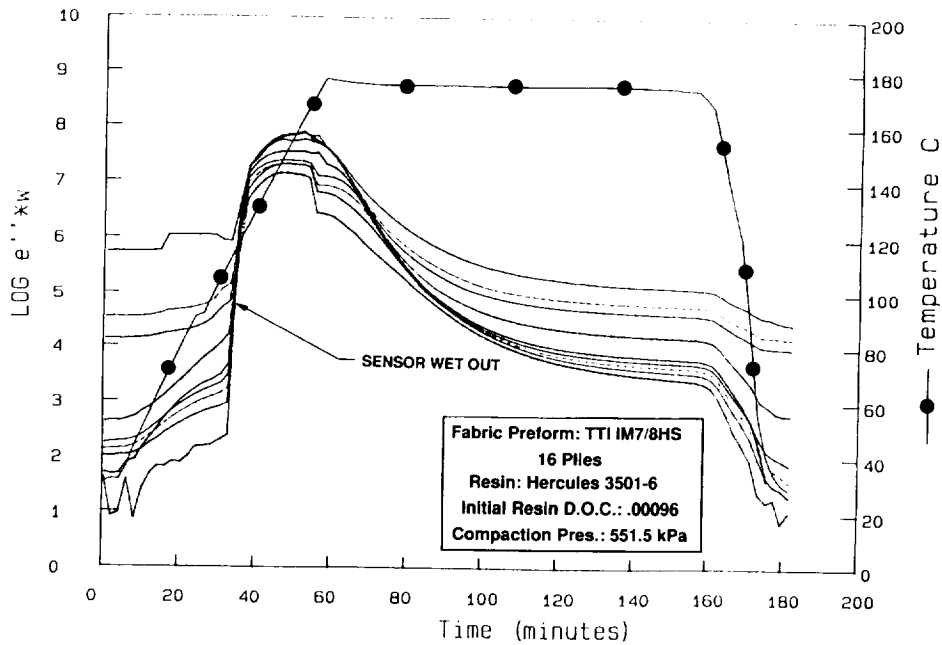


Figure 8. Values of  $\epsilon''$  multiplied by frequency ( $\epsilon'' \cdot \omega$ ) for the top sensor. Constant frequency lines plotted from bottom to top are 50 Hz, 125 Hz, 250 Hz, 500 Hz, 5 kHz, 25 kHz, 50 kHz, 0.25 MHz, and 0.50 MHz. Wet out of sensor occurs at 36 minutes.

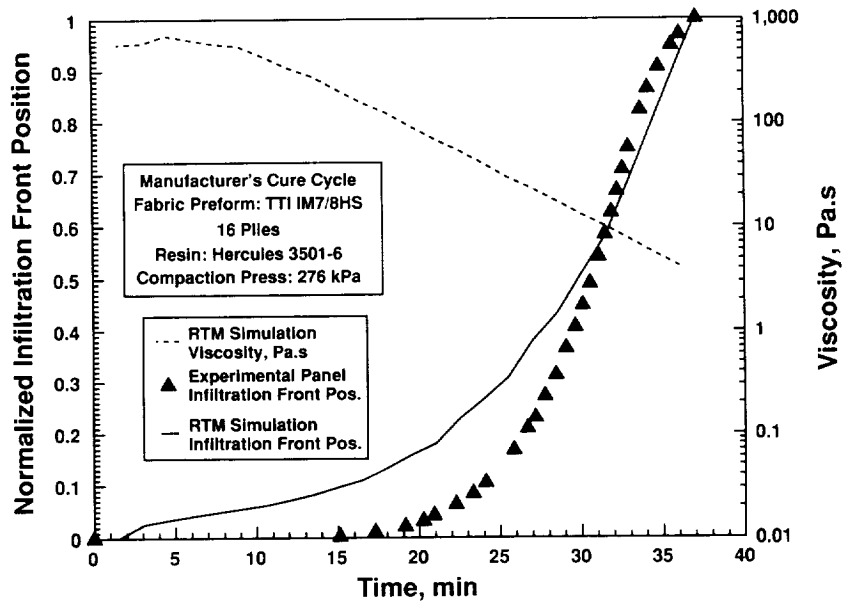


Figure 9. Normalized infiltration front as a function of time.

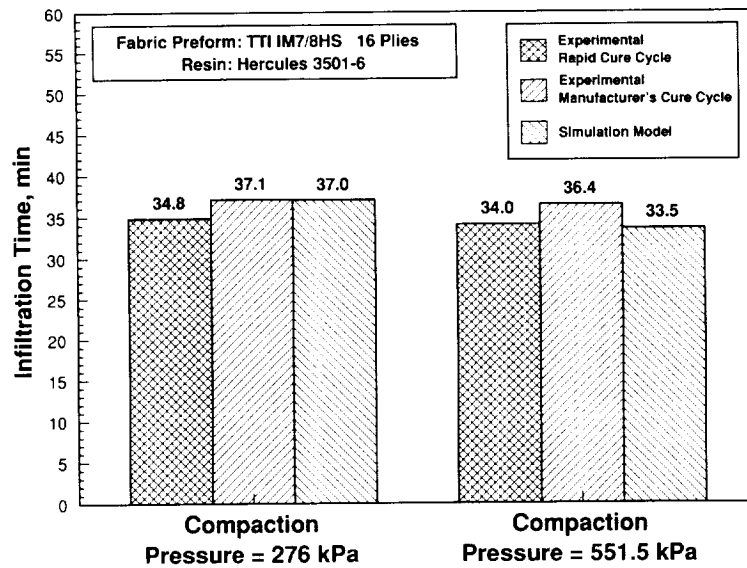


Figure 10. Comparison between measured and model calculated infiltration times.

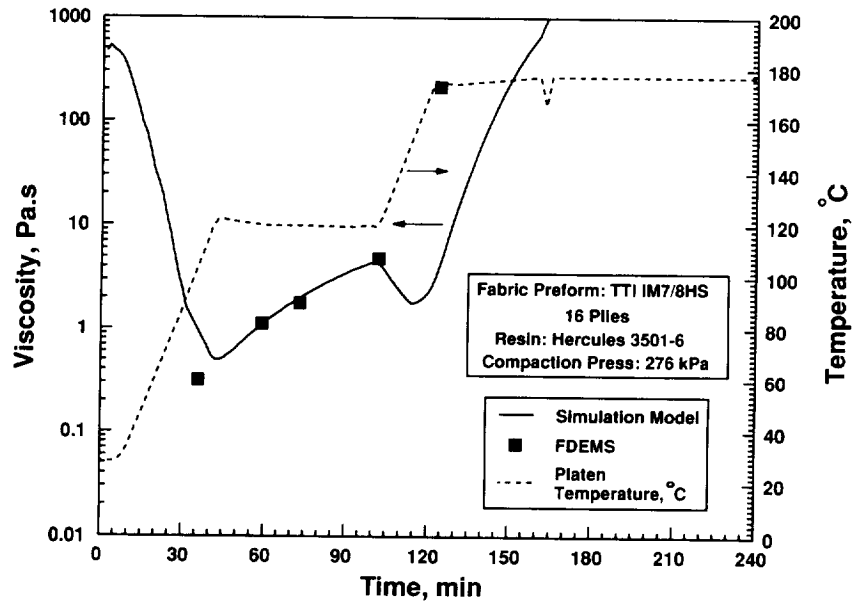


Figure 11. Resin viscosity as a function of time at the bottom of the fabric preform. Comparison between FDEMS measured and model calculated values of resin viscosity.

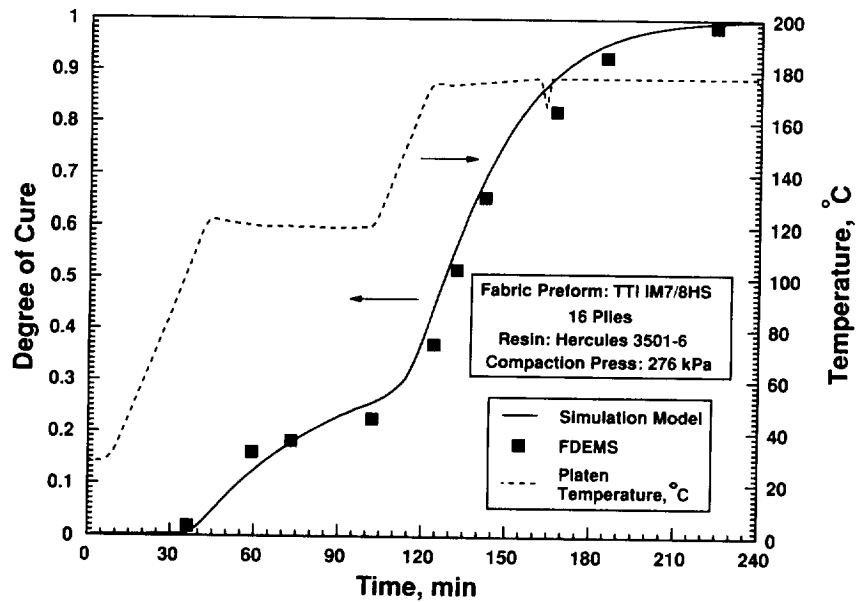


Figure 12. Resin degree of cure as a function of time at the bottom of the fabric preform. Comparison between FDEMS measured and model calculated values of resin degree of cure.

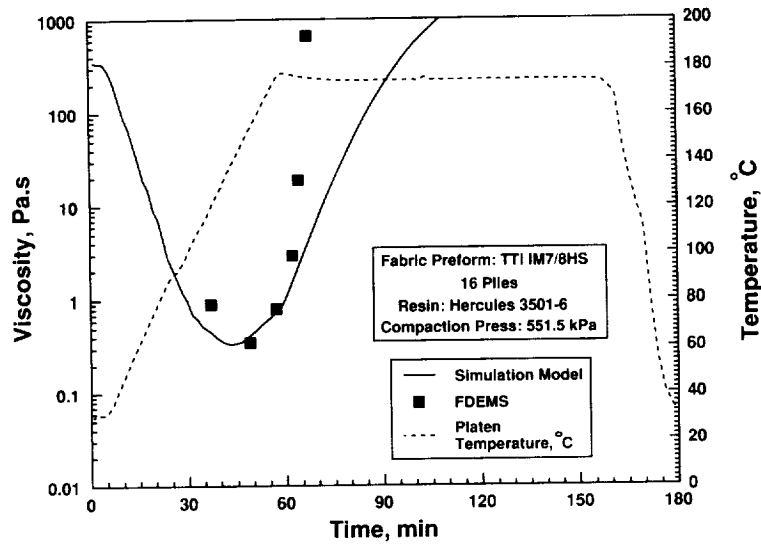


Figure 13. Resin viscosity as a function of time at the bottom of the fabric preform. Comparison between FDEMS measured and model calculated values of resin viscosity.

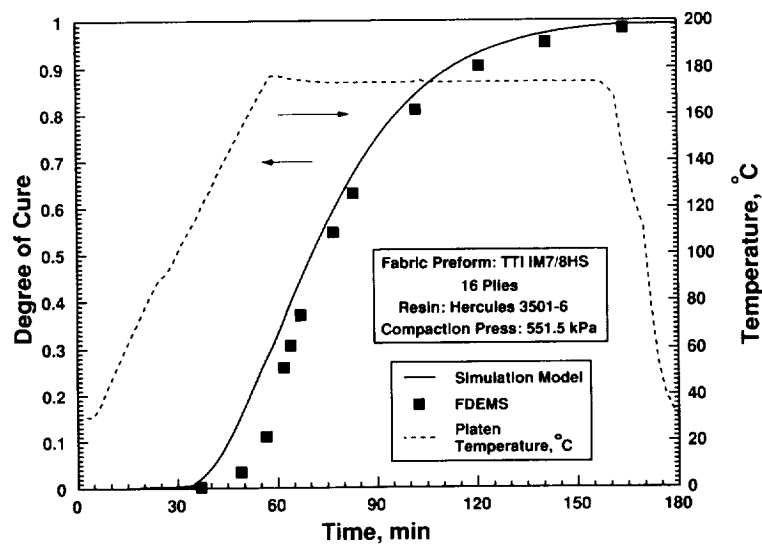


Figure 14. Resin degree of cure as a function of time at the bottom of the fabric preform. Comparison between FDEMS measured and model calculated values of resin degree of cure.

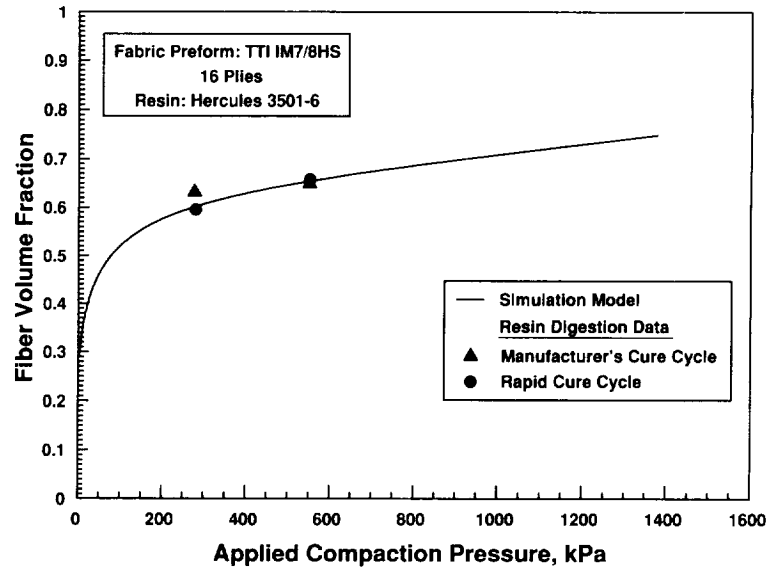


Figure 15. Fiber volume fraction as a function of compaction pressure.

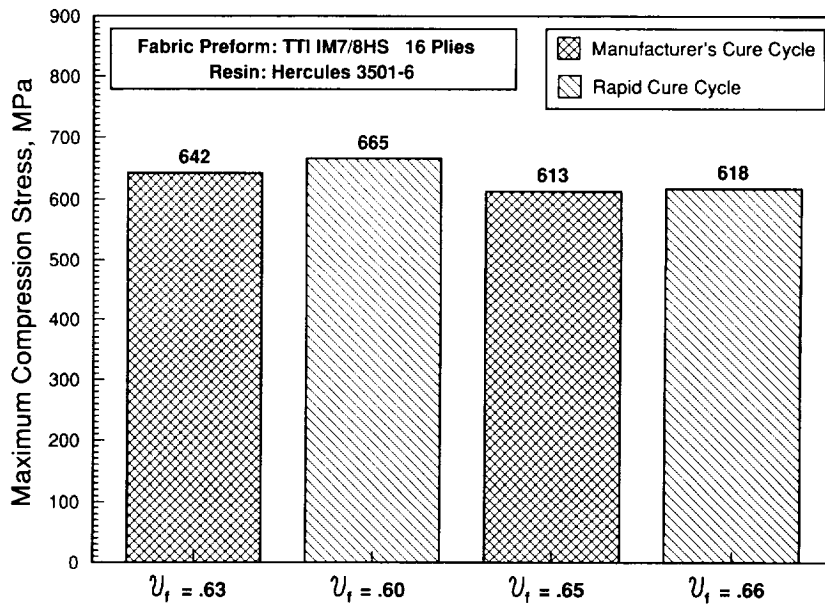


Figure 16. Maximum compression stress for IM7/8HS fabric preforms infiltrated and cured using different compaction pressures and thermal cure cycles.

